Proceedings of the
Annual Stability Conference
Structural Stability Research Council
Baltimore, Maryland, April 10-13, 2018

A partial-distributed damage method for progressive collapse of 3D steel composite buildings

Fani Derveni[1], Panos Pantidis[2], Simos Gerasimidis[3], Kara D. Peterman[4]

Abstract
The present paper studies the response of a 3D steel composite building to progressive collapse through the Partial Distributed Damage Method (PDDM). The method can assess the robustness of 3D steel and concrete composite structures, considering the introduction of partial damage to more than one element in contrast to the dominant Alternate Load Path Method (APM) which involves a complete loss of a member. Computational analysis using finite element software ABAQUS is performed, in order to account for the instability phenomena and assess the integrity of the structure. Considering a damage degree index δj, PDDM predicts lower and more critical collapse loads in comparison with APM.

1. Introduction

Progressive collapse is a catastrophic failure, partial or total, that propagates from the localized damage caused by an event. Blast loads, terrorist attacks, fire, gas explosions or vehicle collisions can be the causes of the initial local failure. The terrorist attack in Murrah Building in Oklahoma (1996), the plane collision at the World trade center in New York (2001) and the bombing of the Khubar Tower in Saudi Arabia (1996) are hailed as the instigating failures which highlighted the need for research in progressive collapse.

US Department of Defense (DoD, 2016) and the General Services Administration (GSA, 2013) are the two major documents that provide design recommendations for reducing the potential for progressive collapse. Both documents include the Alternate Load Path Method (APM) as an analysis method. APM has become widely popular in the field since it is based on the simple concept of a key-component removal from the structure and the assessment of the structural integrity of the remaining structure.

Research on progressive collapse has been multi-faceted during the last decades. Ettouney et al. (2006) and Kwasniewski (2010) applied the APM in two-dimensional frames and in three-

[1] Graduate Research Assistant, University of Massachusetts, Amherst, <fderveni@umass.edu>
[2] PhD Candidate, University of Massachusetts, Amherst, <ppantidis@umass.edu>
[3] Assistant Professor, University of Massachusetts, Amherst, < sgerasimidis@umass.edu >
[4] Assistant Professor, University of Massachusetts, Amherst, < kpeterman@umass.edu >

dimensional structures respectively, in order to assess the response of the buildings under a column loss scenario. Adopting the APM, analytical methodologies were applied in Gerasimidis (2014) and Pantidis and Gerasimidis (2017) that indicate the collapse modes and the critical collapse loads of 2D moment resisting frames for the case of an external column removal and an interior column loss, respectively.

Alashker et al. (2011), in a study of composite floor systems and their shear connections, concluded that the steel deck provides the most significant contribution and as a result, planar simulations are unconservative. Li and El-Tawil (2014), focused on the role of the slab in the robustness of the structure in a suite of 3D nonlinear simulations. Pantidis and Gerasimidis (2018) captured the collapse mechanisms activated by an interior key-component removal via analytical and numerical models of a 3D composite building and denoted failures as either yielding type or stability type.

Agarwal and Varma (2014) evaluated the response of the buildings subjected to fire, while Gerasimidis et al. (2017) investigated the post-fire response until the overall collapse. While column loss as described in APM can reduce complexity in progressive collapse analyses, failure of a member throughout its whole length and the assumption of negligible damage to other components is unrealistic and unconservative, as described in Ellingwood (2002). Blast events were evaluated in McConnell and Brown (2011) and Mlakar et. al. (1998) concluded that damage can be distributed to more than one element and that the complete removal notion utilized in APM is unconservative.

Therefore, partial distribution of damage is needed to gain insight in progressive collapse. Partial Distributed Damage Method (PDDM) was introduced by Gerasimidis et al. (2013), in which a model of a short steel frame with partial column losses predicted no significant instability phenomena. Gerasimidis and Sideri (2016) applied PDDM in a 15-story 2D moment resisting frame. Through 165 damage scenarios they observed the collapse mechanisms of the building, while they identified more critical collapse loads than APM.

The current study implements the Partial Distributed Damage Method in a 9-story 3D steel and concrete composite building. Local damage is distributed to adjacent columns in the first floor of the structure through damage indices δ_j. Advanced computational analysis is performed, and loss of stability phenomena are captured accurately. Lower buckling loads are predicted in comparison with the widely used APM. The advantage of the method is that it constitutes a more realistic scenario than a complete member loss and it is able to assess the global robustness of the structure.

2. Partial-distributed damage method (PDDM) description

The distribution of damage degree in the proposed method is based on the indices δ_j introduced by Kachanov, as shown in Eq. 1:

$$\delta_j = \frac{A - A'}{A}, 0 \leq \delta_j \leq 1 \quad (1)$$

where A is the overall area of each element j and A′ is the effective resisting area. The method relies on the assumption that the introduction of damage to a member leads to a decrease in cross

sectional area, and an increase in its effective stress. Effective stress (Eq. 2) and effective area (Eq.3) are formulated in terms of δ_j as follows:

$$\sigma' = \frac{\sigma}{1 - \delta_j} \tag{2}$$

$$\{A\}' = \{A\}(1 - \delta_j) \tag{3}$$

In this study damage is distributed between an interior and a next-to-exterior column.

A set of six damage scenarios are introduced in the first floor of the structure, including five partial distributed damage scenarios and 1 complete column removal one.
The notation depicted in Table 1 is used to describe each damage scenario (DS):

Table 1: Damage Distribution between columns C3 and B3

Damage Scenario	Damage Indices	Cross-sectional Area decrease
DS(1)	δ_j^A=1	Complete Loss
	δ_j^B=0	No Damage
DS(2)	δ_j^A =0.9	10%A
	δ_j^B=0.1	90%A
DS(3)	δ_j^A =0.8	20%A
	δ_j^B=0.2	80%A
DS(4)	δ_j^A =0.7	30%A
	δ_j^B=0.3	70%A
DS(5)	δ_j^A=0.6	40%A
	δ_j^B=0.4	60%A
DS(6)	δ_j^A =0.5	50%A
	δ_j^B=0.5	50%A

where δ_j=1 corresponds to complete column loss (fully damaged element) and δ_j=0 to a fully intact column (no damage). Any other value of δ_j in the range (0,1) corresponds to partial damage. The equivalence of the partial distribution of damage (PDDM) and the complete removal scenarios (APM) is established in Eq. 4, which allows for meaningful comparisons between the two methods:

$$\delta_j{}^A + \delta_j{}^B = 1 \tag{4}$$

3. Progressive collapse capacity and critical loads

Critical collapse loads are calculated at each damage scenario produced by vertical push-down static analysis. As Pantidis and Gerasimidis (2018), Pantidis and Gerasimidis (2017) and Gerasimidis (2014) found that the governing collapse mechanism was stability-type failure in the lower stories, this work focuses on the distribution of damage in the first floor of the building, expecting a stability-related collapse mechanism. For the analysis performed in this paper, the expected collapse mechanism is a column buckling failure. However, the method can be account for other collapse mechanisms as well.

The governing equation used for the prediction of the Collapse Load (CL) at each separate damage scenario is:

$$CL(k) = max\{CL_I(k), CL_{II}(k)\} \quad (5)$$

where k= 1,2, …,6 and refers to each Damage Scenario, while CL_I and CL_{II} corresponds to Analysis I and Analysis II as described below:

- Analysis I: A push-down analysis is performed, and first column buckling occurs at a collapse load $CL_I(k)$.
- Analysis II: The buckled column is then removed from the structure, and a second push-down analysis is performed. The remaining elements in the model maintain their initial damage state and a collapse load CLII(k) is predicted, when a second column is buckling.

The final collapse load is defined using Eq. 5, as the maximum of the two buckling loads obtained from analyses I and II.

Failure propagates to the structure in two possible ways as described below:

1. Case I: If the applied load that causes the first column buckling $CL_I(k)$ is lower than the applied load $CL_{II}(k)$ at which second column buckles, the failure propagation is initiated in the first analysis and it is progressing in the second. Therefore, $CL_{II}(k)$ identifies the ultimate collapse capacity of the structure.
2. Case II: If the applied load $CL_I(k)$ of the first buckled column is higher than the applied load $CL_{II}(k)$ of second buckled column, the collapse capacity is governed by the first analysis. That means that the second failure occurs immediately after the first buckling failure and hence $CL_I(k)$ is able to provoke both buckling failures.

4. Modelling and Numerical Application

4.1 Prototype structure description

The current work adopts the 9-story Boston Pre-Northridge building designed by the Federal Emergency Management Agent (FEMA 2000) and used by Foley et al. (2007). The building is a 5-bay building with each bay spanning 9.144m. Gravity load is applied with identical loads at all floors above the column removal. Bolted double angle connections are adopted, and a non-linear tension and compression response of each bolt-element is defined according to Shen and Astaneh-Asl (2000), Liu and Astaneh-Asl (2000) and Thornton (1985). Furthermore, as per Pantidis and Gerasimidis (2018), the compression zone is modeled bilinearly with a perfectly plastic branch. In tension the capacity drops to zero after the limit state is attained.

4.2 Finite Element approach

The prototype structure is simulated using the advanced finite element software ABAQUS Simulia (2014), as depicted in Fig 2. Beam elements are used for all the beams and columns, with a three-dimensional beam element with two integration points (B32OS). Warping of open sections is considered. Each column is comprised of 10 elements, while each primary girder is comprised of 18 elements and each secondary beam is comprised of 20. S4 elements are used for modeling the slab, which involves a shell element with a four-node integration. The mesh of the slab follows the

mesh of the beams so that the nodes between the slab and the beams are merged reflecting composite action.

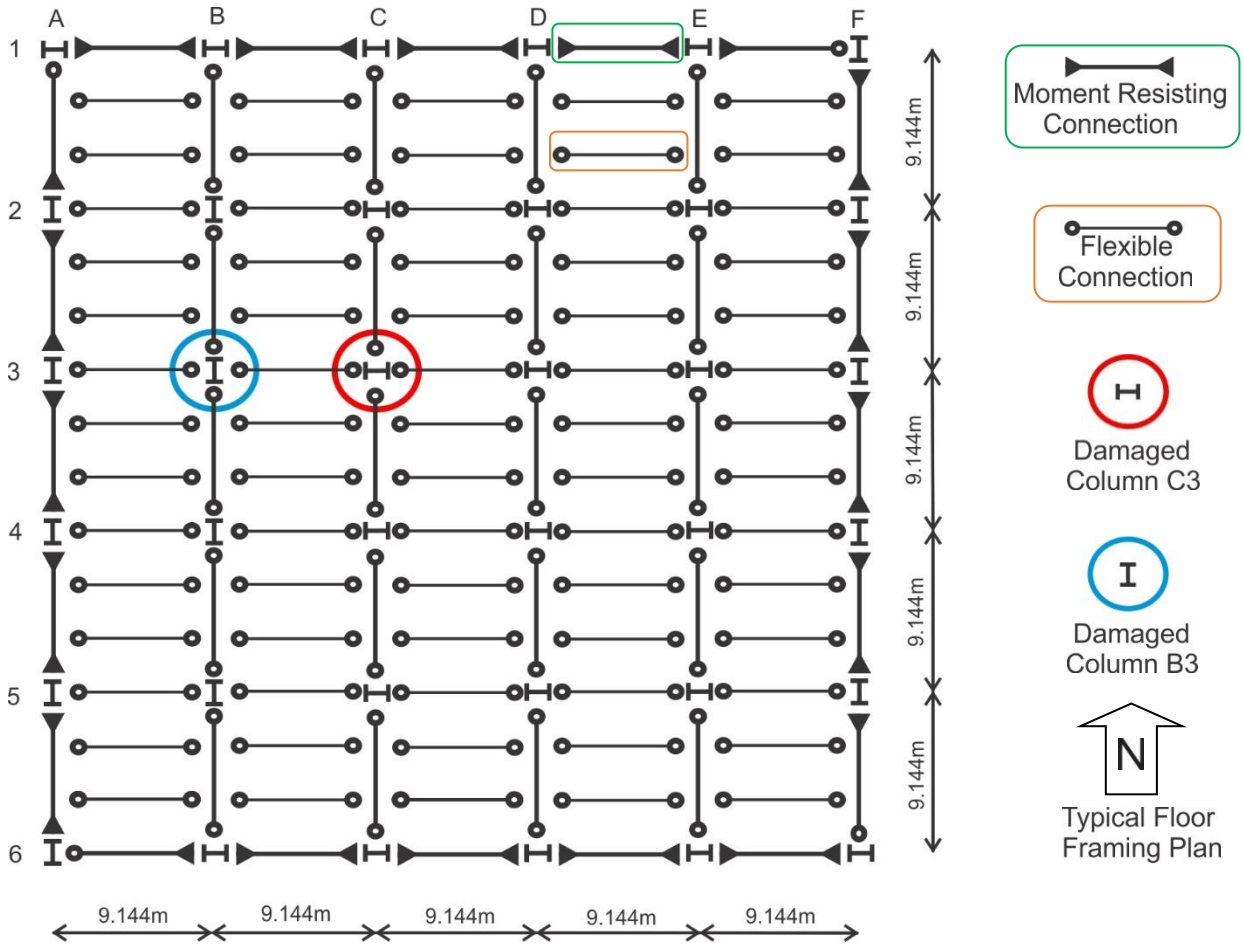

Figure 1: Plan view of the Boston North Pre-Northridge 10-story building. Highlighted columns C3 and B3 in which damage is introduced

Typical steel properties are used for the beams and columns, with a modulus of elasticity of 210GPa, a material yield stress of 345MPa and an ultimate stress of 448MPa at a strain of 18%, with isotropic strain hardening. The slab has a typical concrete material with a modulus of elasticity of 20GPa and a compressive strength of 20MPa, while Concrete Damaged Plasticity model is used for simulating the tension and compression characteristics of the concrete. 2VLI22 steel deck contributes to the tensile capacity of the slab, having a bilinear perfectly plastic material branch and collaborating with the 6x6-W1.4xW1.4 wire mesh for the increase of the capacity of the slab.

Perimeter moment resisting frames are assumed to behave rigidly, while the interior gravity connections are modeled using the CONN3D2 connector element from the ABAQUS library. In particular, SLOT and ROTATION options are chosen for the connector element and ELASTICITY and FAILURE options are used for describing their axial loading properties.

Full modeling description, design considerations and assumption clarification can be found in Pantidis and Gerasimidis (2018).

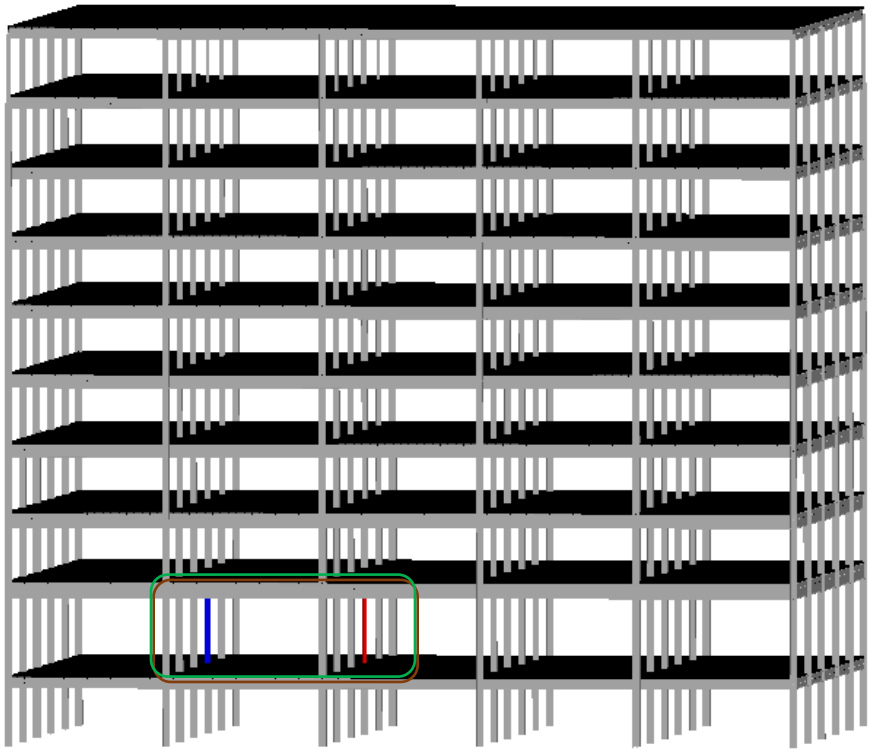

Figure 2: Finite Element simulation in ABAQUS of the 3D steel and concrete composite structure. Damage distribution between columns C3 and B3 in the first floor of the building

5. Results and Discussion

Table 2 shows a full presentation of the collapse loads estimated by the finite element analysis. The final collapse capacity of both analyses in each damage scenario is highlighted.

Table 2: Collapse Loads and Ultimate Collapse Capacity at each Damage Scenario

Damage Scenario		C3 Collapse Load	B3 Collapse Load
DS(1), C3 Removal (APM)	Analysis I	-	9.24 kPa
	Analysis II		
DS(2), δ_j^{C3}=0.9; δ_j^{B3}=0.1	Analysis I	1.44 kPa	
	Analysis II	-	8.40 kPa
DS(3), δ_j^{C3}=0.8; δ_j^{B3}=0.2	Analysis I	2.64 kPa	
	Analysis II	-	7.30 kPa
DS(4), δ_j^{C3}=0.7; δ_j^{B3}=0.3	Analysis I	3.80 kPa	
	Analysis II	-	6.30 kPa
DS(5), δ_j^{C3}=0.6; δ_j^{B3}=0.4	Analysis I	5.00 kPa	
	Analysis II	-	5.50 kPa
DS(6), δ_j^{C3}=0.5; δ_j^{B3}=0.5	Analysis I	6.30 kPa	
	Analysis II	-	4.60 kPa

- DS(1), Full Column Removal Scenario - APM, (δ_j^{C3}=1; δ_j^{B3}=0):
  The first damage scenario comprises of the full removal of the interior gravity column C3, as shown in Fig. 3(a). In this case, the immediate adjacent column B3 has an abrupt, brittle horizontal displacement, which displays its inelastic buckling failure. The applied load at which buckling is happening is 9.24kPa. A second analysis is not needed in this scenario, since the absence of two columns is considered as a state of structural collapse. As a result, the collapse load in this damage scenario is CL(1)=9.24kPa. Fig. 3(b) depicts the Von-Mises stresses throughout the B3 column cross section until the column buckles. The five section integration points across the width of the column are illustrated in the graph. The green line represents the stress in the column fiber which is closer to the removal, while the blue line depicts the stress in the other outer fiber. The rest stresses lie in between the outer fibers.

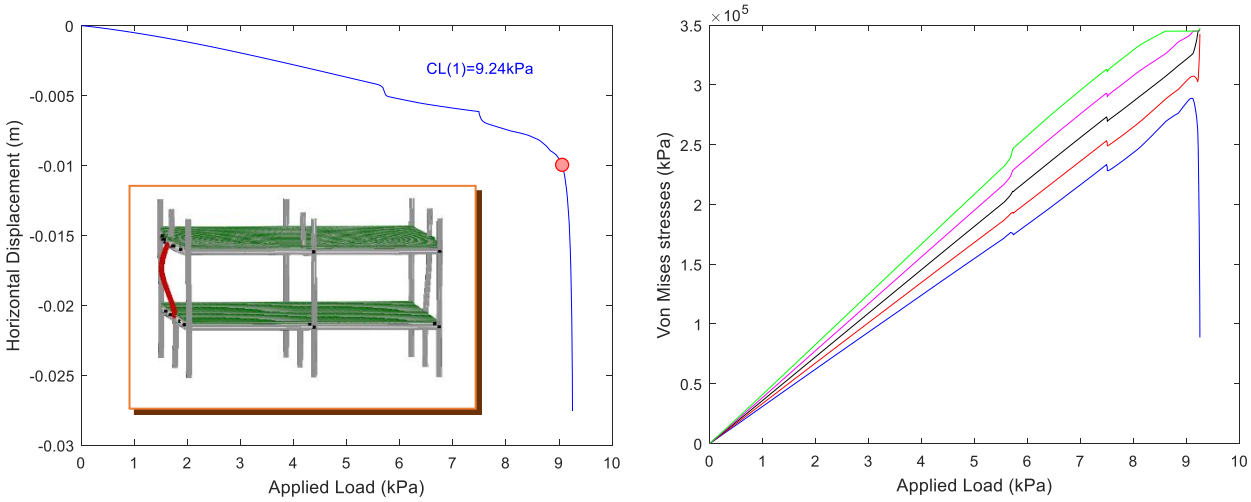

Figure 3: Complete Column C3 Removal (Alternate Load Path Method). (a) Horizontal Displacement of column B3 against applied load. (b) Von-Mises Stresses of the I-cross section points against applied load. The column section has non-uniform compressive stresses.

- DS(2), Partial Distributed Damage, (δ_j^{C3}=0.9; δ_j^{B3}=0.1):
  This damage scenario involves of the partial distribution of damage between C3 and B3 columns. In particular, 90% of the damage is introduced in C3 column, while 10% of the damage is assigned in B3. In the proposed method, that means that the 10% of the cross sectional area of C3 and the 90% percent of the cross sectional area of B3 contribute in this analysis. In the first analysis, C3 buckling failure is observed at $CL_I(2)$=1.44kPa. At this point column C3 reaches its inelastic capacity. In the second analysis, column B3 reaches its axial capacity at $CL_{II}(2)$=8.4kPa.

  The final collapse load is calculated using Eq. 5 as CL(2) = max {CLI(2),CLII(2)}=8.4kPa. The results of this damage scenario are shown in Fig. 4. It must be mentioned that the collapse capacity is decreased by 9% in comparison with the APM column removal scenario described previously. This is a first significant finding that illustrates that PDDM leads to more critical collapse loads than APM.

- DS(3) and DS(4), Partial Distributed Damage, (δ_j^{C3}=0.8; δ_j^{B3}=0.2 and δ_j^{C3}=0.7; δ_j^{B3}=0.3):
  In the following 2 damage scenarios, the same tendency is observed in the results. Specifically, the first analysis predicts lower collapse loads of C3 column buckling ($CL_I(3)$=2.64kPa and $CL_I(4)$=3.8kPa) than the second analysis of B3 column buckling failure ($CL_{II}(3)$=7.3kPa and $CL_{II}(4)$=6.3kPa).

  Therefore the final collapse loads for DS(3) and DS(4), in which the axial capacity is reached and the columns cannot withstand any additional axial force, are CL(3)=7.3kPa and CL(4)=6.3kPa, respectively. The axial forces in the columns in every damage scenario tend to increase linearly until the inelastic buckling occurs. The collapse capacity is decreased by 21% in DS(3) and by 32% in DS(4) in comparison with the APM column removal scenario.

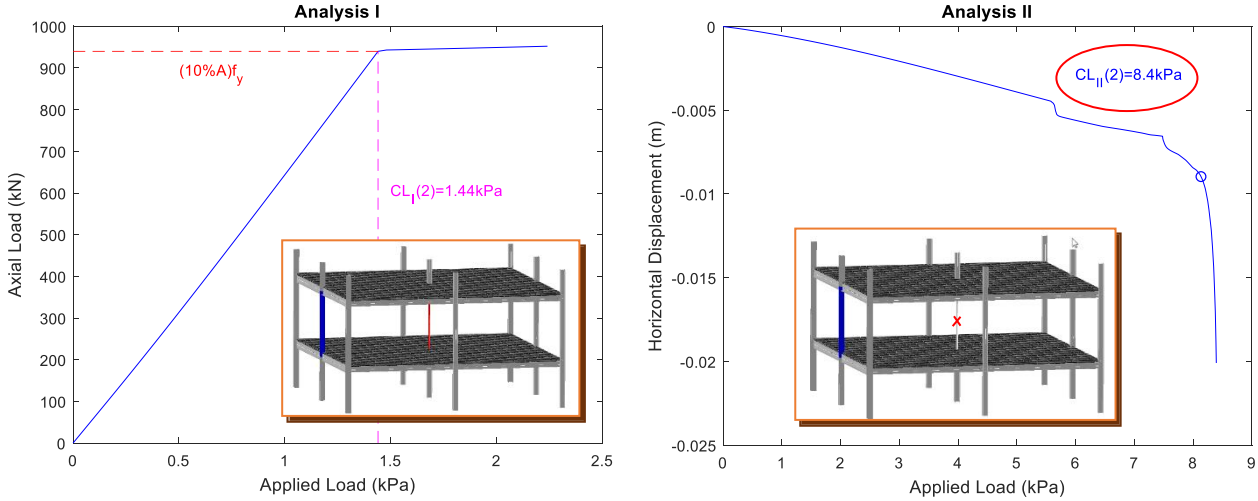

Figure 4: Damage Scenario DS(2), δ_j^{C3}=0.9; δ_j^{B3}=0.1: (a) Axial Load of Column C3 against collapse load in the first analysis, (b) Abrupt Horizontal Displacement of column B3 against collapse load in the second analysis

- DS(5), Partial Distributed Damage, (δ_j^{C3}=0.6; δ_j^{B3}=0.4):
  This damage scenario results to a $CL_I(5)$=5kPa when column C3 buckles and $CL_{II}(5)$=5.5kPa when column B3 buckles, illustrate the second column buckling almost at the same collapse. The collapse capacity at this scenario is CL(5)=5.5kPa and compared to the APM of DS(1) it is 41% smaller.

- DS(6), Partial Distributed Damage, (δ_j^{C3}=0.5; δ_j^{B3}=0.5):
  The cross sectional area assigned in columns C3 and B3 are equal and as a result their inelastic capacity is the same. The first analysis displays the C3 column buckling at the vertical load of $CL_I(6)$=6.3kPa, while second analysis leads to B3 buckling failure at the collapse load of $CL_{II}(6)$=4.6kPa, as illustrated in Fig. 5. In this case, the second buckling failure happens immediately after the first one. The collapse capacity is CL(6)=6.3kPa and it is 32% smaller in comparison with the APM of DS(1).

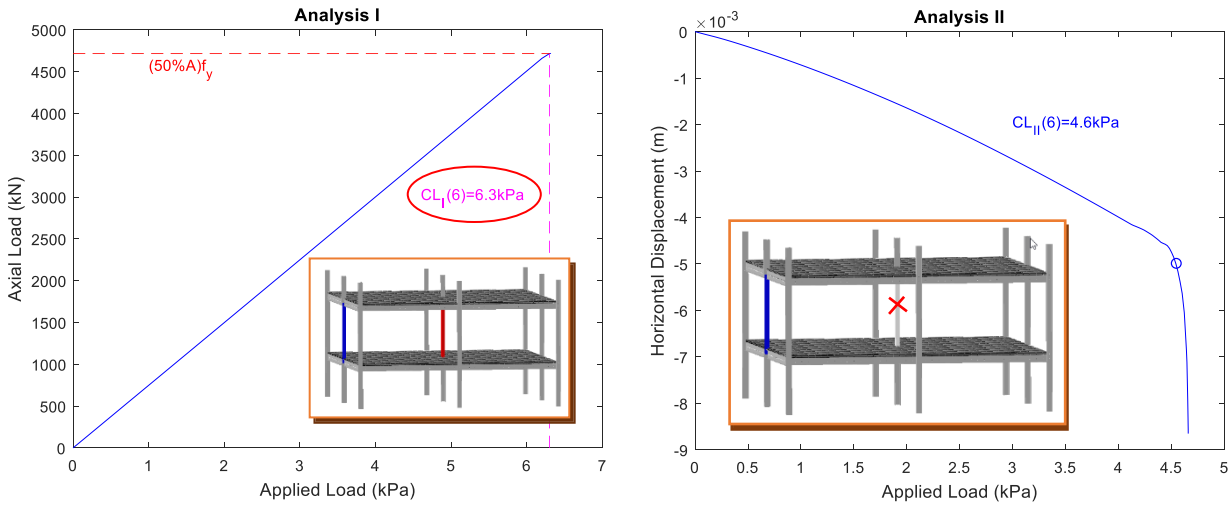

Figure 5: Damage Scenario DS(6), δ_j^{C3}=0.5; δ_j^{B3}=0.5: (a) Axial Load of Column C3 against collapse load in the first analysis, (b) Abrupt Horizontal Displacement of column B3 against collapse load in the second analysis

The most significant finding of these analyses is that Partial Distributed Damage Method predicts lower collapse loads than Alternate Load Path Method. Fig. 6 illustrates the collapse loads of each partial distributed damage scenario normalized by the collapse load of the notional element removal scenario (APM). The discrepancy between the two methods are highlighted in the graph and a high decrease in the collapse load is observed. Hence the collapse capacities predicted by the proposed method are considered more critical for progressive collapse analysis.

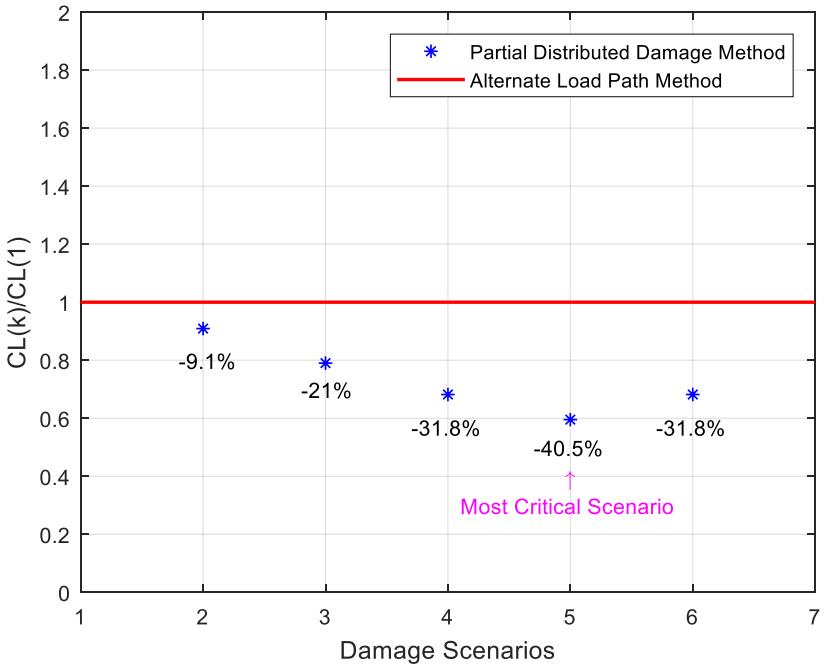

Figure 6: Collapse Loads against Damage Scenarios. Comparison between Partial Distributed Damage Method (PDDM) and Alternate Load Path Method (APM). More critical buckling loads are evaluated, and discrepancy percentages are pointed in the graph.

Another important finding is the correlation of the resulting collapse loads with the progressive collapse design load of the building, according to DoD (2016). The vertical Design Load (DL) is:

$$DL = 1.2D + 0.5L \tag{6}$$

where D is the dead gravity load of 4.6kPa and L is the live load of 2.39kPa. The applied design load equals 6.71kPa. Based on the results attained by the finite element analysis, it turns out that PDDM predicts lower loading resistance than the progressive collapse design loading combination from DoD (2016), as depicted in Fig. 7. Although APM would not require any progressive collapse design for the specific structure, the results from PDDM show that the capacity is not enough for some partial damage scenarios. This raises concerns about the APM.

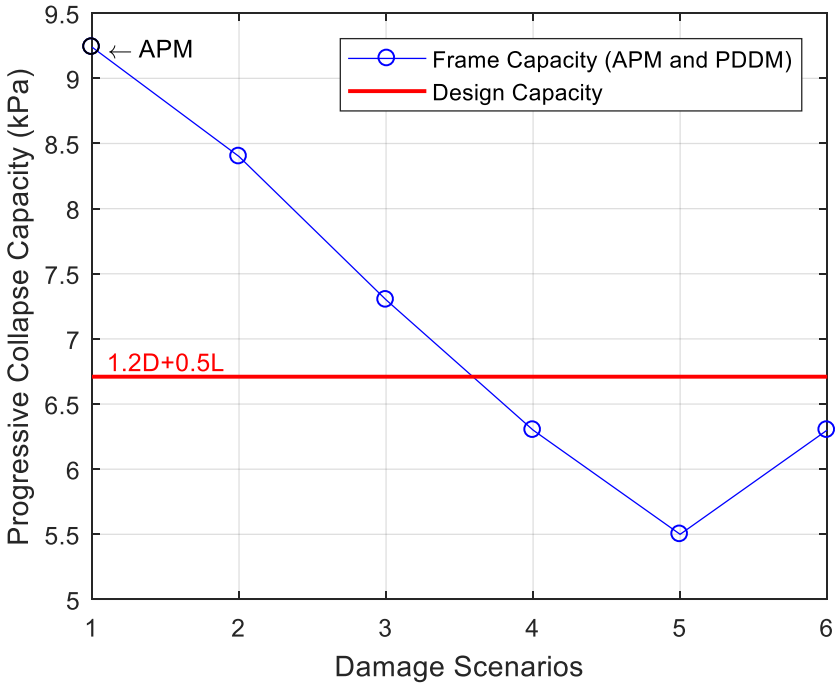

Figure 7: Progressive collapse capacity predicted by the analysis against damage scenarios (DS). Partial Distributed Damage Method displays more critical resistance capability of the structure than the calculated design load.

6. Conclusions

This work sheds light on the response of steel composite buildings under extreme loading events through Partial Distributed Damage Method (PDDM). Different ratios of damage were applied to elements of the structure and the buckling loads as well as the overall collapse capacities were evaluated.

The two most important findings of the proposed method are:

1. Lower buckling loads and therefore more critical ultimate collapse capacities are predicted by PDDM in comparison to APM. The discrepancy between the methods can be high in some cases. For example, DS(5), which introduces 60% of the damage in column C3 and the remaining 40% in column B3, demonstrated that PDDM analysis yields a decrease of 40.5% in collapse load, when compared to total column removal. Hence the APM can overpredict the capacity of the structure.

2. In some damage ratios, lower collapse capacity is predicted, as compared to the required progressive collapse design capacity of the structure. DS(1) which represents the APM has a safety factor of 1.38 against the DoD (2016) design load combination. DS(4) and DS(5) however have safety factors of 0.94 and 0.82 respectively.

References

DoD (2016). Unified Facilities Criteria (UFC), "Design of buildings to resist progressive collapse". Washington, DC: Department of Defense.

US General Service Administration (GSA); 2013. "Alternate path analysis & design guidelines for progressive collapse resistance".

Ettouney, M., Smilowitz, R., Tang, M., & Hapij, A. (2006). Global system considerations for progressive collapse with extensions to other natural and man-made hazards. *Journal of performance of constructed facilities*, *20*(4), 403-417.

Kwasniewski, L. (2010). Nonlinear dynamic simulations of progressive collapse for a multistory building. *Engineering Structures*, *32*(5), 1223-1235.

Gerasimidis, S. (2014). Analytical assessment of steel frames progressive collapse vulnerability to corner column loss. *Journal of Constructional Steel Research*, *95*, 1-9.

Pantidis, P., & Gerasimidis, S. (2017). New Euler-Type Progressive Collapse Curves for Steel Moment-Resisting Frames: Analytical Method. *Journal of Structural Engineering*, *143*(9), 04017113.

Alashker, Y., Li, H., & El-Tawil, S. (2011). Approximations in progressive collapse modeling. *Journal of Structural Engineering*, *137*(9), 914-924.

Li, H., & El-Tawil, S. (2013). Three-dimensional effects and collapse resistance mechanisms in steel frame buildings. *Journal of Structural Engineering*, *140*(8), A4014017.

Pantidis, P., & Gerasimidis, S. (2018) Loss-of-stability vs yielding-type collapse mode in 3D steel structures under a column removal scenario: an analytical method of assessing the collapse mode.

Agarwal, A., Varma, A.H. (2014). "Fire induced progressive collapse of steel building structures: the role of interior gravity columns", *Engineering Structures*, 58: 129-140.

Gerasimidis, S., Khorasani, N. E., Garlock, M., Pantidis, P., & Glassman, J. (2017). Resilience of tall steel moment resisting frame buildings with multi-hazard post-event fire. *Journal of Constructional Steel Research*, *139*, 202-219.

B.R. Ellingwood, Load and resistance factor criteria for progressive collapse design, 2002. (Available from http://www.nibs.org).

McConnell, J. R., & Brown, H. (2011). Evaluation of progressive collapse alternate load path analyses in designing for blast resistance of steel columns. *Engineering Structures*, *33*(10), 2899-2909.

Mlakar, Sr, P. F., Corley, W. G., Sozen, M. A., & Thornton, C. H. (1998). The Oklahoma City bombing: analysis of blast damage to the Murrah Building. *Journal of Performance of Constructed Facilities*, *12*(3), 113-119.

Gerasimidis, S., Bisbos, C. D., & Baniotopoulos, C. C. (2013). A computational model for full or partial damage of single or multiple adjacent columns in disproportionate collapse analysis via linear programming. *Structure and Infrastructure Engineering*, *10*(5), 670-683.

Gerasimidis, S., & Sideri, J. (2016). A new partial-distributed damage method for progressive collapse analysis of steel frames. *Journal of Constructional Steel Research*, *119*, 233-245.

Kachanov, L. (1986). Introduction to continuum damage mechanics, *Springer, Brookline, MA*.

FEMA-355C (2000). State of the art report on systems performance of steel moment frames subject to earthquake ground shaking, Washington DC: Federal Emergency Management Agency.

Foley, C., Martin, K., Schneeman, C. (2007). "Robustness in structural steel framing systems", Final Report submitted to American Institute of Steel Construction, Inc. Chicago, IL.

Shen, J., Astaneh-Asl., A. (2000). "Hysteresis model of bolted-angle connections", *Journal of Constructional Steel Research*, 54: 317-343.

Liu, J., Astaneh-Asl, A. (2000). "Cyclic testing of simple connections including effects of slab", *Journal of Structural Engineering*, 126(1): 32-39.

Thornton, W.A. (1985). "Prying action – A general treatment", *Engineering Journal*, Second Quarter, American Institute of Steel Construction, Chicago, IL, 67-75.

Manual, Abaqus User. (2014). "Abaqus Theory Guide. Version 6.14." *USA.: Dassault Systemes Simulia Corp*.